Accepted Manuscript

Development of electric resistance sintering process for the fabrication of hard metals: Processing, microstructure and mechanical properties

M.A. Lagos, I. Agote, T. Schubert, T. Weissgaerber, J.M. Gallardo, J.M. Montes, L. Prakash, C. Andreouli, V. Oikonomou, D. Lopez, J.A. Calero

PII: S0263-4368(17)30055-0
DOI: doi: 10.1016/j.ijrmhm.2017.03.005
Reference: RMHM 4426

To appear in: *International Journal of Refractory Metals and Hard Materials*

Received date: 31 January 2017
Revised date: 7 March 2017
Accepted date: 12 March 2017

Please cite this article as: M.A. Lagos, I. Agote, T. Schubert, T. Weissgaerber, J.M. Gallardo, J.M. Montes, L. Prakash, C. Andreouli, V. Oikonomou, D. Lopez, J.A. Calero , Development of electric resistance sintering process for the fabrication of hard metals: Processing, microstructure and mechanical properties. The address for the corresponding author was captured as affiliation for all authors. Please check if appropriate. Rmhm(2017), doi: 10.1016/j.ijrmhm.2017.03.005

DEVELOPMENT OF ELECTRIC RESISTANCE SINTERING PROCESS FOR THE FABRICATION OF HARD METALS: PROCESSING, MICROSTRUCTURE AND MECHANICAL PROPERTIES

M.A. Lagos[1], I. Agote[1], T. Schubert[2], T. Weissgaerber[2], J.M. Gallardo[3], J.M. Montes[3], L. Prakash[4], C. Andreouli[5], V. Oikonomou[5], D. Lopez[6], J.A. Calero[6]

[1] TECNALIA RESEARCH & INNOVATION

[2] Fraunhofer Institute for Manufacturing Technology and Advanced Materials IFAM, Branch Lab Dresden

[3] University of Seville

[4] KYOCERA UNIMERCO TOOLING AS

[5] MIRTEC

[6] ALEACIONES DE METALES SINTERIZADOS (AMES)

ABSTRACT

This work presents the development of the Electrical Resistance Sintering (ERS) process for the fabrication of Hard Metals. The compositions of the materials produced were WC with 6 and 10 wt % of Co. In addition to the specific characteristics of the technology, the characterization of the produced parts is presented and compared to materials obtained by conventional processes.

The parts produced by ERS present densities comparable to the ones obtained by conventional methods. The microstructural comparison shows a considerable grain size reduction in the ERS materials which consequently brings a hardness increase. ERS materials show similar fracture toughness to conventional ones.

The very fast sintering allows performing the process without any protective atmosphere, therefore making this process very attractive for the production of materials that need to be sintered under non-oxidising environments. The total duration of the cycle, including heating, holding time and cooling is few seconds.

Finally, some considerations about the scale up and possible industrialization of the technology are explained.

Keywords: Electrical sintering, ERS, FAST, cutting tools, tungsten carbide

1. INTRODUCTION

ECAS (electric current assisted sintering) gathers a family of consolidation methods in which mechanical pressure is combined with electric and thermal fields to enhance particle bonding and densification. The primary purpose of imposed electric current is to provide the required amount of resistive heat. The expression field-assisted sintering techniques (FAST) have become also popular in literature to denominate these technologies. Indeed, the speed of the processes is the most remarkable characteristic and the common factor among these techniques.

ECAS techniques can be classified with respect to the processing time [1]. In conventional ECAS processes, like SPS (Spark Plasma Sintering) [2], low current densities and voltage are applied (typically < 10 V and 1 kA/cm^2). With these conditions, processing time is in the range of minutes and for that reason a controlled atmosphere is needed. However, in very fast processes like EDS (Electro Discharge Sintering) [3] and ERS (Electric Resistance Sintering) [4-6] higher current densities are applied (typically > 5 kA/cm^2) and the processing time is few seconds. The short duration of the cycle permits the processing in air without any protective atmosphere. This is a very important advantage from the economic point of view. In EDS, the electric discharge is produced with a high-voltage

capacitor bank, whereas in ERS the current is produced by a low-voltage transformer (around 10 V). Therefore, the current applied to the sample is easier to control in ERS and this improves the homogeneity of the products.

Electrical resistance sintering (ERS), was already described in 1933 by Taylor [7] and later modified by Cremer [8] in 1944. However, up to now, the ERS process has been used for the consolidation of high conductive materials (pure metals) at lab scale, obtaining very small pieces [4-6]. The development of medium voltage machines (40 V) opens the possibility of obtaining larger parts and using materials with lower electrical conductivity like composites and cermets.

WC–Co cemented carbides have been widely used for cutting tools of various materials and other machine parts which are required to show high resistance to frictional wear. Their mechanical properties can be modified over a broad range by changing the content of the binding Co phase and the WC grain size [9-13]. Cemented carbides are usually produced by sintering with the participation of a liquid cobalt phase. However, the presence of this phase during the WC–Co sintering, stimulates the growth of the WC grains. In general, with decreasing WC particle size properties such as hardness, wear resistance, and transverse rupture strength of the composite are improved [14-16]. The effect of the nanostructure in the WC-Co carbides properties has been extensively studied [17-19]. It is known that fracture toughness decreases with increasing hardness in conventional composites, whereas the increase of hardness in nano-structured composites does not further reduce their bulk fracture toughness. This implies that different dominant toughening mechanisms exist in the conventional and nanostructured composites. Very fast sintering processes offer a unique opportunity to avoid the liquid phase sintering and thus limit the grain growth.

This paper presents the development of the ERS technology for the processing of hard metals. The new pilot plant scale equipment is shown. An electric press of 15 t was combined with medium voltage transformers in a fully automated ERS equipment.

Microstructural and mechanical characterization of the materials are presented and compared to commercial sinter-hipped carbides. In addition, some important aspects of the technology are described.

2. MATERIALS AND METHODS

WC-Co powders (submicron size) were used with the following composition: 6 wt% of Co and 10 wt% of Co. Granulated powders from a commercial source were procured with organic wax and a pre-treatment was performed in order to eliminate organic components. The spherical morphology of the granules with a size between 100-200 µm can be observed in Figure 1A. Each granule is composed of very fine powder (size less than 1 micron). The surface of one granule is observed in Figure 1 B. Apparent density of the granulated powder was 3,7 g/cm^3.

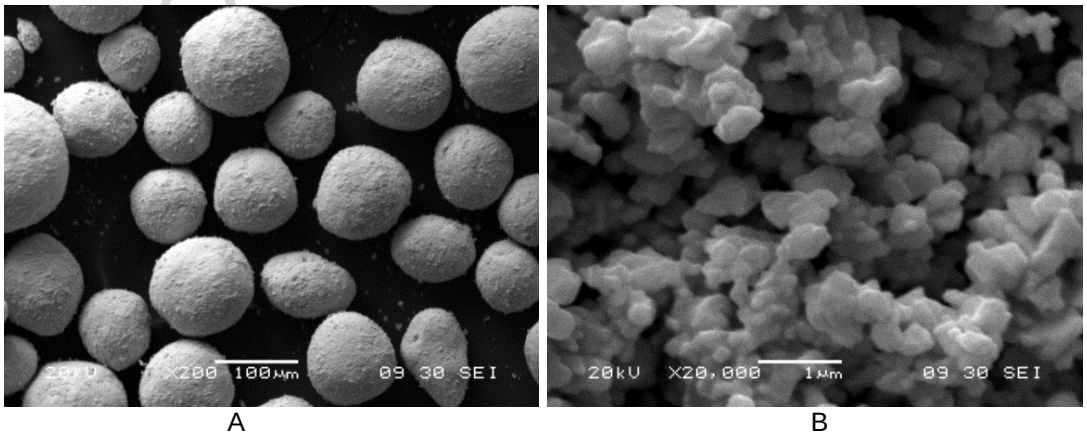

A B

Figure 1. WC-6Co powder, A) SEM image of the granulated powder, magnification X200, B) SEM image of the surface of the granules, magnification X20000.

For the ERS processing, the powder was filled in an alumina based ceramic die between two copper electrodes (see the diagram of the ERS machine in Figure 2A). The dimensions of the produced parts were 22 mm in diameter with a thickness of 10-14 mm. The maximum applied current density was between 4-5 kA/cm^2 with a holding time of 500 ms. Maximum load was 100 MPa. An image of the prototype machine used in this work is presented in Figure 2B. This fully automated ERS machine was developed within the EU funded EFFIPRO project. Maximum voltage of the machine is 40 V with a maximum current of 35 kA. The pressure is applied using a 15 tones electrical press.

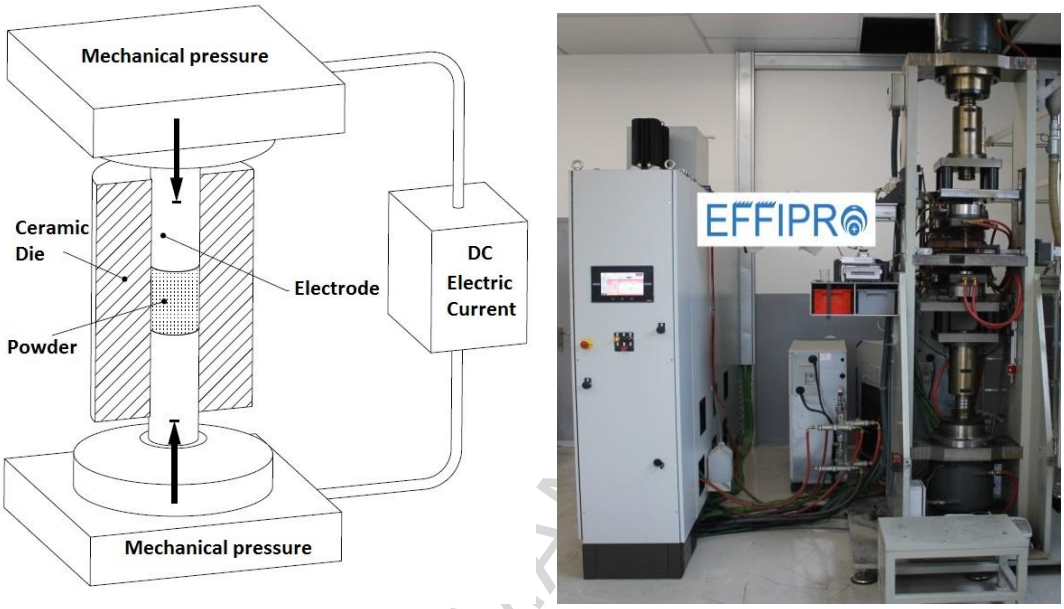

A B

Figure 2. A) Diagram of the technology, B) Prototype machine, developed within the EFFIPRO project

Density was measured by Archimedes method using a Mettler AE 240 weight balance and porosity was analysed according to the standard UNE-EN ISO 4605:1978. Microstructure and semi-quantitative chemical composition were analysed by optical and SEM microscopy (Zeiss Nvision 40 and Zeiss EVO50). Hardness Vickers (HV30) was measured according to the standard UNE-EN ISO 6507-1:2006. KIC was calculated from the length of the radial cracks originated in the corners of the Vickers indentations according to the formula proposed by Shetty et al. [20]. The analysis of the magnetic coercivity HC and saturation magnetisation MS was performed according to DIN ISO 3326 using a Koerzimat CS 1.096, from Förster GmbH. The W content of the Co binder was calculated from measurements of magnetic moment [21]. Measurement of lattice parameter of the Co binder phase was made with an X-ray diffractometer using CuKα radiation on the surface of test-pieces which were electrolytically etched to remove WC. The electrolyte consisted of 4-mol solution of NaOH in reagent grade.

3. RESULTS AND DISCUSION

3.1. Characteristics of the ERS processing for the fabrication of WC-Co

Figure 3 shows the clear relationship between the current applied and the global density obtained in the ERS samples, measured by the Archimedes method. Increasing the density of current, the global density of the samples is increased. The material with 10 % of Co presented better results of densification compared to the material with 6 % of Co.

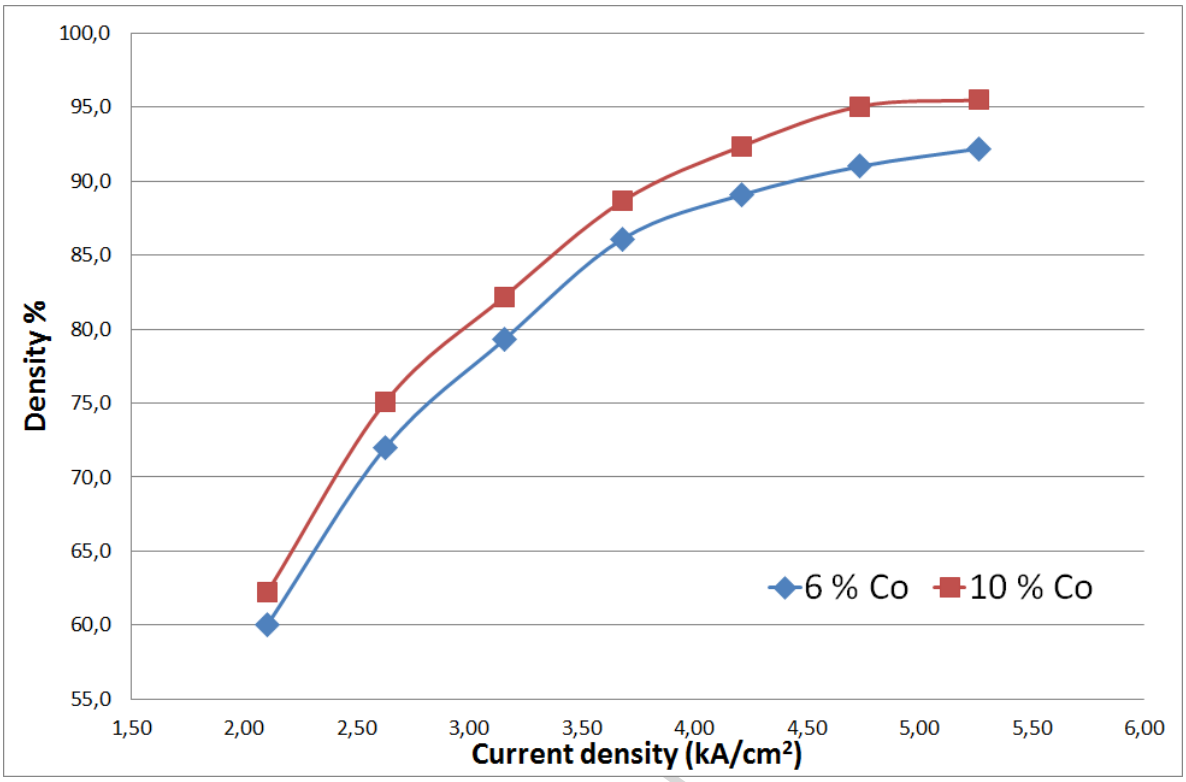

Figure 3: Relationship between the density and the electric current applied (density includes the external porous layer; core of the samples was fully dense)

The ERS samples typically consist of a dense core surrounded by a porous surface layer as it is shown in Figure 4A. The density values presented in figure 3 show values between 90 and 95% of the theoretical density due to the fact that the outer porous layer is included. It has been observed that increasing the current density, the area of the external porous layer decreases. The thickness of the outer porous layer in contact with the metallic punches (top and bottom of the sample) is thinner than that in contact with the ceramic die walls (see figure 4B and 4C). After removing this layer, samples obtained using ERS show very high density, within typical required values for hard metal tools. Porosity at the core is very low (A02 according to the standard UNE-EN ISO 4605:1978).

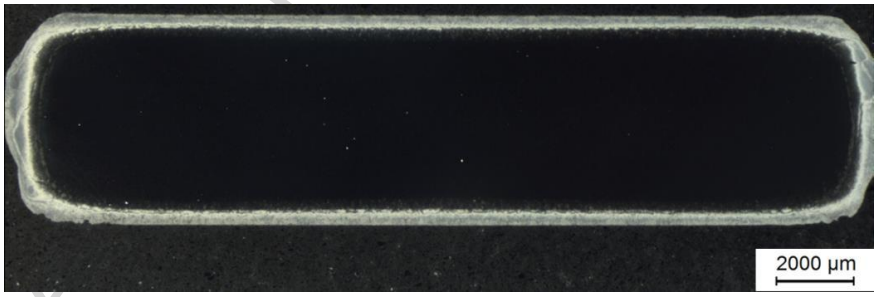

A

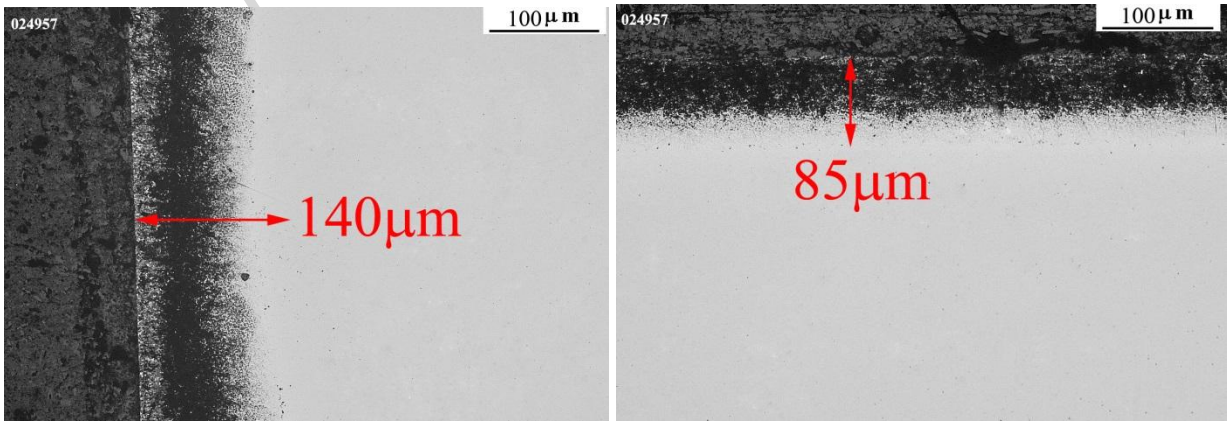

B C

Figure 4. Cross section of a part produced by ERS, distribution of the porosity: A) Whole sample, B) External porosity, contact with the punches (scale bar 100 microns), C) External porosity, contact with the ceramic die (scale bar 100 microns)

In ERS process, the electrical current passes across the material and the heating is produced by joule's effect. Temperature in the material depends on different factors. One of the most important ones is the green density distribution of the parts. It is known that in a double sided pressing, green density of the parts is lower at the core. Where porosity is higher, electrical resistance is also higher. This fact produces higher temperature at the core of the material during resistance heating. Another important factor is the heat losses produced by conduction from the material to the dies and electrodes; this also increases the temperature gradient from the core of the parts to the borders. For that reason, external porosity is produced by the fast cooling of the material in contact to the copper punches and ceramic die. Based on preliminary experimental data, it seems that it is possible to improve this phenomenon reducing the external porosity by using ceramic dies with lower thermal conductivity.

3.2. Microstructural characterization of the products

Microstructures of the materials obtained by ERS are shown in Figure 5 (6 and 10 % Co). In both cases microstructure is composed of polygonal WC grains surrounded by Co metallic matrix (darker in the images).

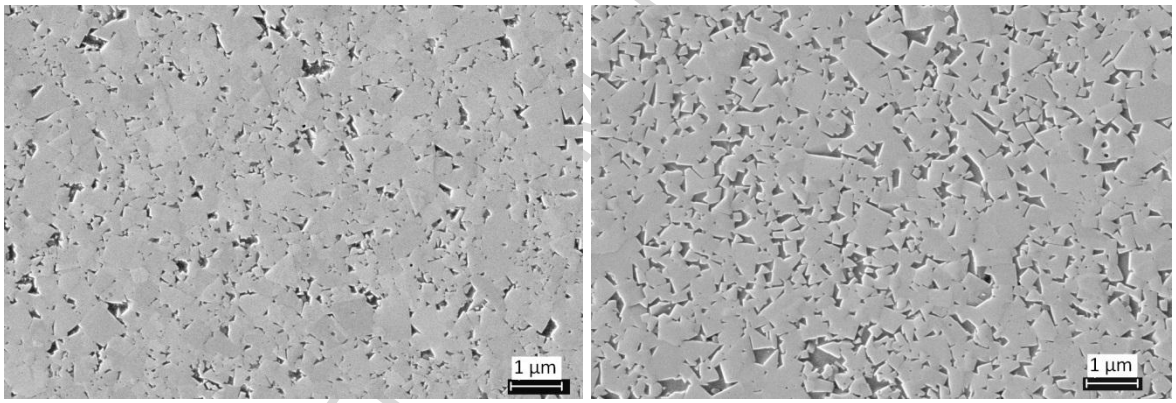

Figure 5. HRSEM images of polished cross sections of ERS/WC6Co (left) and ERS/WC10Co.

In addition, Figure 6 presents for comparison with conventionally sintered material ion-etched cross sections of materials with 6 % of Co obtained by ERS and Sinter HIP, using in both cases the same starting powders.

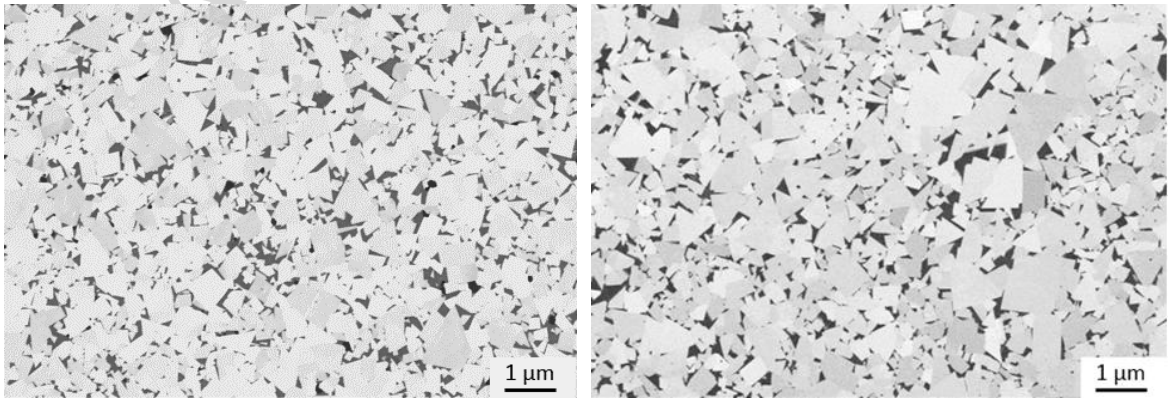

A B

Figure 6. HRSEM images of polished and ion-etched cross sections of ERS/WC6Co (A) and Sinter HIP material (B)

Crystal grain size was estimated by the linear intercepts method (based on DIN EN 623-3). This method is based on the number of average lengths of intercepts through each crystal/grain along a line drawn across the material surface. The measured lengths of intercepts for WC and the Co binder of WC6Co are given in Table 1. The real phase sizes are about 1.4x larger than the measured intercepts owing to the measuring procedure. The measurements of phase sizes were done after an ion etching of the polished sample for improving the image quality. The measured lengths of intercepts for WC give a WC-grain size of about 274nm for ERS and 326nm for the conventional process. The reason for this very low grain growth are the very short processing time and very fast cooling rate during the ERS process. The size of the Co phase is similar in the conventional and ERS processes.

Table 1. Comparison of phase sizes of differently processed hardmetal WC6Co

Process	*Phase*	*Length of intercepts (nm)*			*Number of measured regions*
		d_{10}	$\boldsymbol{d_{50}}$	d_{90}	
ERS	WC	73	**196**	441	934
	Co	28	**73**	218	310
Sinter-HIP	WC	89	**233**	528	932
	Co	28	**77**	195	417

Comparing these results with previous literature, grain size obtained in ERS samples is similar to the one reported by Spark Plasma Sintering of nanocrystalline powders [22]. It is important to take into account that in the present work submicron powders were used instead of nanometric ones. The very low grain growth observed during processing opens the possibility of nano-crystalline hard metals.

The contiguity of ERS WC6Co was measured with about 67% WC/WC combined with 33% WC/Co boundaries. The corresponding values of contiguity for the Sinter-HIP samples were 56% WC/WC and 44% WC/Co. Contiguity decreases with increasing binder content and is also dependent on the processing history of the carbide [23-24]. It is difficult to determine the effect of contiguity on the mechanical properties due to the influence of other microstructural characteristics; however, it is believed that hardness increases with increasing contiguity [24].

Regarding the crystallographic phases, Figure 7 presents the XRD patterns for samples with 10 % of Co.

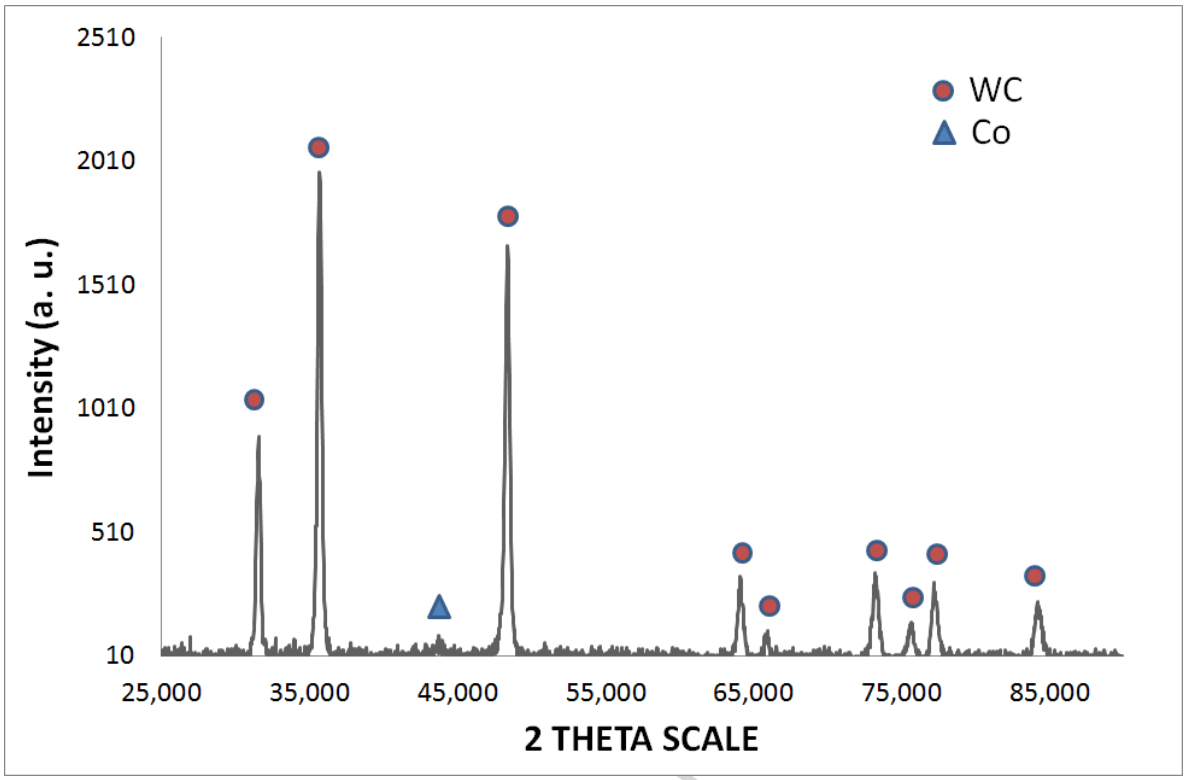

Figure 7. XRD pattern, samples obtained by ERS, WC -10Co

The revealed main phases are WC-hexagonal and Co-cubic; traces of Co-hexagonal were also detected in both samples.

Measurements of lattice parameter of the Co binder phase were made on the surface of test-pieces which have been electrolytically etched to remove WC. From the XRD measurements lattice parameters of Co were calculated and the concentration of W and C in the binder were estimated. The lattice parameter of the fcc phase can be expressed as [21]:

$$a = a_o + Q \cdot mw + R \cdot mc$$

where a_o, Q and R are constants with values of 0.3548 nm, 0.00036 and 0.0012, respectively. The atomic percentages of W and C are given by mw and mc respectively. Obtained values are presented in Table 2.

3.3. Mechanical properties

Materials obtained by ERS (6 and 10 % Co) presented higher hardness compared to conventional materials obtained by Sinter-HIP (see Table 2). A hardness increase of the 5 % was observed for the 6 % Co and and increase of the 8 % for the 10 % Co.

Table 2. Summary of properties of differently processed hard metals

Composition	*Process*	*Density (g/cm^3)*	*Hardness HV30*	*Fracture toughness K_{1C} ($MPa\sqrt{m}$)*	*H_C (Oe)*	*M_S (10^{-7} $T*m^3*kg^{-1}$)*	*Co binder composition (wt%) W*	*Co binder composition (wt%) C*
WC6Co	ERS	14.7	1960±15	9.6±0.5	470	101	9.8	0.04
	Sinter-HIP	14.8	1860±15	9.5±0.5	385	103	8.8	0.03
WC10Co	ERS	14.3	1750±20	10.3±0.5	420	150	9.0	0.14
	Sinter-HIP	14.4	1620±15	10.2±0.5	320	154	13.9	~0

In ERS materials, a small variation of the hardness was observed between the core and the surface of the samples, presenting a small increase of the hardness at the surface. This phenomenon is not completely clear at the moment. This can be linked to a slightly higher grain size observed at the core of the samples. Samples are heated by Joule's effect during ERS and the temperature at the core of the samples is slightly higher than at the surface. This longer time at high temperature can produce a very small increase in grain size. Another possible explanation is the migration of Co from the core of the samples; this migration can produce small micro-porosity and the local decrease of the hardness. However, not significant variations in the Co content were observed.

The applicability of the Hall-Petch equation for hardness predictions:

$$H = E_1 + F_1 . d_{WC}^{-1/2}$$

has been examined for materials with nominally 6 wt% Co (approximately 10 vol%). H is the hardness and dwc the grain size (WC arithmetic mean linear intercept). E_1 and F_1 are constant values. Least squares regression analysis was used to fit a linear plot to the data with values for the constants E_1 and F_1 of 913 and 601, respectively. The hardness measured on the ERS samples does not meet the mentioned correlation (see Figure 8); the prediction should produce a higher hardness as measured based on an intercept of 200nm. Therefore, it is not clear, if this relationship between hardness and WC grain size can further be extended to the ultrafine grades.

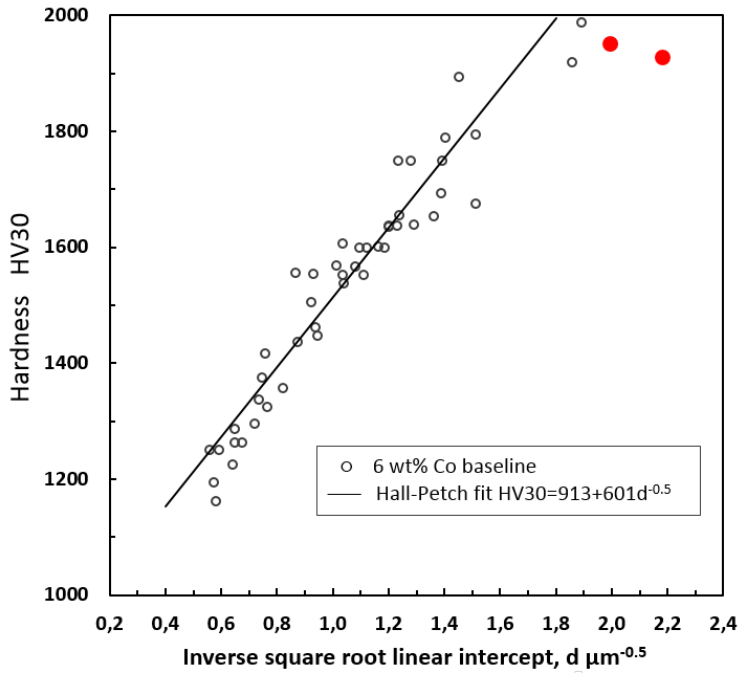

Figure 8. Relationship between hardness and grains size. ERS materials marked as red circles [21]

Fracture toughness (K_{1c}) reveals similar behaviour for the differently processed samples (conventional and ERS) with values in the range of 9-10 MPa $m^{0.5}$ (see table 2). It is known that fracture toughness decreases with increasing hardness in conventional composites, whereas the increase of hardness in nano-structured composites does not further reduce their bulk fracture toughness [17-19]. The very short processing time used in ERS (in the orders of few seconds) helps controlling the grain growth and thus obtaining finer microstructures. It is believed that this reduction in grain size increases the hardness but maintaining the fracture toughness constant.

The microstructural characterisation of the WC–Co hardmetals is often performed using magnetic measurements. By measuring the magnetic saturation MS or the coercivity HC, it is possible to obtain an approximation of the WC grain size, cobalt content and even determine the presence of additional phases. Generally, an increase of coercivity is observed with a decrease in WC grain size. The comparison of the measured H_C values of ERS with Sinter-HIP samples confirms the reduction in grain size observed in ERS materials.

A relationship between magnetic coercivity and arithmetic mean linear intercept is given in [21], which shows a plot of the coercivity values against grain size for 6 wt% Co hardmetals. These results can be characterised by a straight line given by:

$$K = a + b\, d_{WC}^{-1}$$

where K is the coercivity in kA m^{-1}, a and b are constants and d_{WC} is the WC arithmetic mean linear intercept in µm. The H_C values measured on both fine-grained hardmetal variants show lower coercivities as predicted by the given relationship. It is necessary to be aware that the coercivity also varies with carbon content and W content of the binder-phase. The estimated chemical composition of the Co binder is also shown in Table 2. It was assumed that the binder-phase is a Co-W-C alloy. In practice other elements can be present, particularly Cr, which can have an effect on the magnetic moment which makes precise calculations difficult. The binders contain W and C in solution. Presence of C does not affect the cobalt magnetic saturation and moment values, but W decreases them. Due to the balance of W and C a loss of carbon increases the W content within Co resulting in reduced magnetic saturations. The measured MS values (Table 2) suggest, that all samples are near the lower C limit, as it is presented in Figure 9.

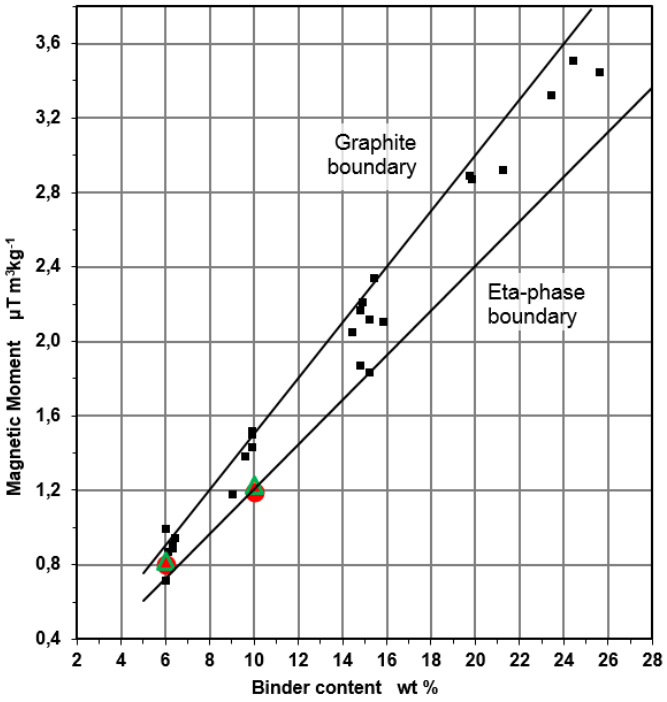

Figure 9. Magnetic moment of different WC/Co hardmetals plotted against Co content [21] compared with the values of the fabricated samples (ERS ●, Sinter-HIP ▲).

4. CONCLUSIONS

In this work, the development of the ERS process for the fabrication of hard metals was presented.

Thanks to the short processing time, the novel sintering technology produced materials with finer grain size than conventional materials. This reduction in grain size increases the hardness of the products maintaining similar fracture toughness.

One of the most interesting advantages of the proposed processing route is the possibility of obtaining near net shape products. For that reason, the production of 2D shapes with greater geometrical complexities was also studied. Figure 10 presents some blanks with complex shapes obtained by

ERS. In addition to the external shape of the blanks, the possibility of internal holes was achieved integrating small inserts within the ceramic dies.

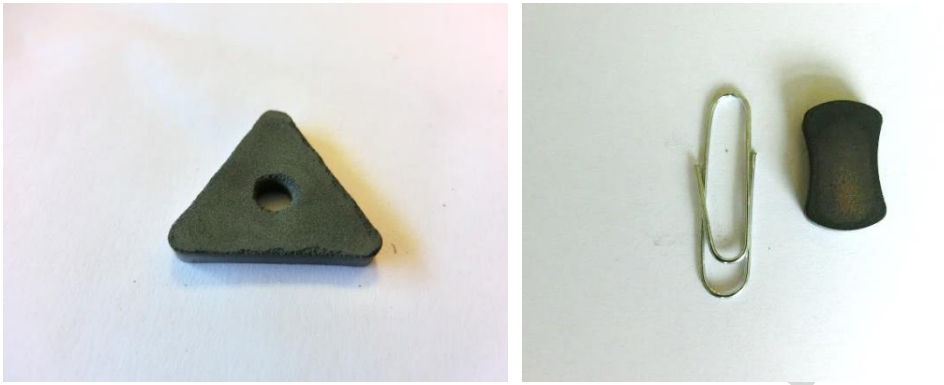

Figure 10. Blanks produced by Hybrid ERS technology

Another important aspect of the technology is the very short processing time with regards to conventional processing. In conventional sintering the duration of the thermal treatment is several hours, in other FAST sintering products like SPS, sintering process is in the range of 20-30 min. In the case of ERS, the processing time is clearly shorter. The pilot plant equipment developed is fully automated and enables the fabrication of around 120-200 blanks per hour.

Regarding the energy consumption, it is true that in the conventional processing, a large number of pieces can be produced in the same cycle and in ERS one piece per cycle is produced. A detailed study of the energy consumption in both cases is needed in order to compare both processes. However, it seems that for small series of pieces and for customized tools, ERS can be an interesting alternative.

5. ACKNOWLEDGEMENTS

This work is financially supported by the Seventh Framework program of the Commission of the European Communities under project EFFIPRO contract no. NMP2-SL-2013-608729.

6. REFERENCES

1. Grasso S, Sakka Y and Maizza G, Electric current activated/assisted sintering (ECAS): a review of patents 1906–2008, Sci. Technol. Adv. Mater, 2009, 10 (Issue 5): 1-24.
2. Anselmi-Tamburini U, Garay, Munir ZA, Fundamental investigations on the spark plasma sintering/synthesis process III Current effect of reactivity. Materials Science and Engineering A, 2005, 407: 24-30.
3. Fais A, Processing characteristics and parameters in capacitor discharge sintering, Journal of Materials Processing Technology, 2010, 210: 2223–2230.
4. J.M. Montes, F.G. Cuevas, J. Cintas, and P. Urban, A One-Dimensional Model of the Electrical Resistance Sintering Process, Metallurgical and Materials Transactions A, Metall and Mat Trans A, 2015, 46: 963.
5. J.M. Montes, J.A. Rodriguez, F.G. Cuevas, J. Cintas, Consolidation by Electrical Resistance Sintering of Ti Powder, Journal of Materials Science, 2010, 46 (15): 5197-5207.
6. Shon J, Park J, Cho K, Hong J, Park N, Oh M, Effects of various sintering methods on microstructure and mechanical properties of CP-Ti powder consolidations, Trans. Nonferrous Met. Soc. China 2014, 24: 59−67.
7. G.F. Taylor: U.S. Patent 1896854, 7 Feb 1933.
8. G.D. Cremer: U.S. Patent 2355954, Aug 1944.
9. Luyckx S, The hardness of Tungsten Carbide-Cobalt hardmetal. In: Riedel R, editor. Handbook of Ceramic Hard Materials, Handbook of Ceramic Hard Materials, Weinheim: Wiley-VCH, 2000, 950-963.
10. Brookes K, World Directory and Handbook of Hard Metals and Hard Materials. 6th edition, Hertfordshire: International Carbide Data, 1996, 83-92.

11. Upadhyaya GS, Materials science of cemented carbides - an overview, Materials and Design, 2001, 22: 483 489
12. Kim BK, Ha GH, Lee DW. Sintering and microstructure of nanophase WC/Co hardmetals. J Mater Process Technol 1997;63:317–21.
13. Teppernegg T, Klünsner T, Kremsner C, Tritremmel C, Czettl C, Puchegger S, Marsoner S, Pippan R, Ebner R, High temperature mechanical properties of WC–Co hard metals, Int. Journal of Refractory Metals and Hard Materials 2016, 56: 139–144.
14. Kim H.C., Shon I.J., Garay J.E., Munir Z.A., Consolidation and properties of binderless sub-micron tungsten carbide by field-activated sintering, International Journal of Refractory Metals & Hard Materials, 2004, 22: 257–264.
15. Kim HC, Shon IJ, Yoon JK, Doh JM, Consolidation of ultra fine WC and WC–Co hard materials by pulsed current activated sintering and its mechanical properties, International Journal of Refractory Metals & Hard Materials 2007, 25: 46–52.
16. X.Y. Wu, W. Zhang, W. Wang, F. Yang, J.Y. Min, B.Q. Wang, and J.D. Guoa), Ultrafine WC-10Co cemented carbides fabricated by electric-discharge compaction, Journal of Materials Research 2004, 19 (8): 2240-2244.
17. Jia K, Fischer TE, Gallois G. Hardness, and toughness of nanostructured and conventional WC–Co composites. Nanostruct Mater 1998;10:875–91.
18. Zhang FL, Wang CY, Zhu M. Nanostructured WC/Co composite powder prepared by high energy ball milling. Scripta Mater 2003;49:1123–8.
19. Shin SG. Experimental and simulation studies on grain growth in TiC and WC-based cermets during liquid phase sintering. Met Mater 2000;6:195–201.
20. Shetty DK, Wright IG, Mincer PN, Clauer AH. Indentation fracture of WC-Co cermets. J Mater Sci 1985;20:1873-82.
21. Roebuck B, Gee M, Bennett EG, Morrell R. Measurement Good Practice Guide No. 20 – Mechanical Tests for Hardmetals, NPL, 1999, ISSN 1368–6550.
22. Cha SI, Hong SH, Kim BK. Spark plasma sintering behavior of nanocrystalline WC–10Co cemented carbide powders. Mater Sci Eng 2003;351:31–8.
23. V.T. Golovchan, N.V. Litoshenko, On the contiguity of carbide phase in WC–Co hardmetals, International Journal of Refractory Metals & Hard Materials 2003, 21: 241–244.
24. S. Luyckx, A. Love, The dependence of the contiguity of WC on Co content and its independence from WC grain size in WC–Co alloys, International Journal of Refractory Metals & Hard Materials 2006, 24: 75–79.

HIGHLIGHTS:

- Development of a new process for the fabrication of hard metals
- Specific characteristics of the technology and about the materials produced
- Microstructural characterization of the obtained products compared to conventional hard metals
- Mechanical and magnetic characterization of the obtained products compared to conventional hard metals
- Practical considerations about the technology regarding processing time and energy consumption